

The Optical Whistle Oscillation: Frustrated Spatial Soliton Formation in Nonlinear Cavities

Jack Boyce and Raymond Y. Chiao

Department of Physics, University of California, Berkeley, California 94720

Voice: (510) 642-5620 Fax: (510) 642-5620

(This version was produced on December 2, 2024)

A new type of transverse instability in dispersively nonlinear optical cavities, called the *optical whistle*, is discussed. This instability occurs in the mean-field, soliton forming limit when the cavity is driven with a finite-width Gaussian beam, and gives rise to oscillation, period doubling, and chaos. It is also seen that bistability is strongly affected due to the oscillation within the upper transmission branch. The phenomenon is interpreted as a mode-mismatch in the soliton formation process and is believed to have broad applicability.

INTRODUCTION

Over the last 25 years the nonlinear optical resonator has been a rich source of interesting phenomena [1]. These systems are attracting attention recently due to their potential applications as all-optical switches, memories [2], and logic gates [3], at both the classical and quantum levels. The resonator geometry naturally gives appreciably stronger nonlinear effects for a given incident beam intensity than do the travelling-wave schemes, potentially allowing the use of faster, less lossy, materials with relatively weaker nonlinearities (for example, atomic vapors or even silica as opposed to thermal or photorefractive materials). The resonator geometry also leads to a variety of time-dependent behaviors which must be adequately characterized, either to avoid undesired effects in engineered systems or to perhaps take advantage of them for communications or computing purposes.

The most fundamental physical process in the nonlinear resonator, plane-wave optical bistability, was first observed experimentally in 1975 [4]. Ikeda [5] later showed in a discrete return-map analysis that as the incident intensity increases the intracavity field intensity can oscillate and undergo a period-doubling route to chaos. In the 1980's a great deal of work concentrated on transverse structure and dynamics in nonlinear cavities, in order to incorporate the phenomena of self-(de)focusing and diffraction. McLaughlin *et al* [6] demonstrated in 1985 that a finite-width Gaussian beam incident on a cavity with a single transverse dimension can give rise to a *transverse* oscillation in the cavity field, essentially due to a modulational instability. These oscillations are of period equal to a multiple of the cavity round-trip time and thus correspond to the occupation of multiple resonator longitudinal modes. More recently Haelterman and Vitrant discussed a transverse oscillation which arises when a nonlinear Fabry-Perot is illuminated obliquely, due essentially to the lateral drift of the field within the cavity [7].

Here we report on the discovery of a new type of oscillation within high-finesse nonlinear cavities driven by Gaussian beams. This *optical whistle* oscillation occurs as a competition between spatial soliton formation [9] [10] and the driving input, and can exhibit regular oscillation or intermittency and chaos. Within the periodic mode the oscillation frequency is roughly proportional to the input field amplitude; the nonlinear cavity acts as a light-controlled RF oscillator.

GENERAL CONSIDERATIONS

The dynamics of a general (dispersively) nonlinear optical cavity driven with a finite-width beam is principally governed by four effects: propagation, damping, diffraction, and nonlinearity. A qualitative understanding of cavity behavior is gained by simply comparing the characteristic timescales of these processes, given by:

$$\begin{aligned}
 \tau_{prop} &= L/c \\
 \tau_{damp} &= L\mathcal{F}/c \\
 \tau_{diff} &= w^2/\lambda c \\
 \tau_{nl} &= \lambda/c\Delta n
 \end{aligned} \tag{1}$$

where L and \mathcal{F} are the cavity length and finesse, λ is the optical wavelength, w is a characteristic size of transverse features in the optical beam, and $\Delta n = |n(I) - n(0)|$ is the typical nonlinear index shift caused by the optical field of typical intensity I (the linear index is assumed to be unity).

The timescale τ_{nl} is the time required for the nonlinearity to induce a 2π phase shift in the light field. For self-focusing nonlinearities we can also identify τ_{nl} as the typical formation time of transverse structure arising from the modulational instability [8]. These structures form with characteristic transverse wavelength $\Lambda = \lambda/\sqrt{\Delta n}$. A feature of this size will diffract apart in a time $\Lambda^2/(\lambda c) \approx \tau_{nl}$, and we generally conclude that these structures spontaneously form so that diffraction and nonlinearity are equally important. The same result applies to the formation of spatial solitons, which can be considered modes of self-induced waveguides [11] [12]. Soliton formation is more efficient when the incident beam is of size Λ , in analogy with mode-matching in linear optics. The optical whistle instability arises from a “mode mismatch” between the beam size and the (self-consistent) soliton dimension Λ .

Returning to the cavity timescales of Eq. 1, one important case is when τ_{prop} is much shorter than the others. In this *mean field limit* the field changes little in traversing the cavity once, and we can suppress the field envelope’s longitudinal dependence. It can be shown [13] that in this limit only a single longitudinal cavity mode is appreciably occupied.

The optical whistle phenomenon exists under the same conditions as spatial soliton formation:

$$\tau_{prop} \ll \tau_{diff} \approx \tau_{nl} \ll \tau_{damp} \quad (2)$$

For the remainder of the discussion we confine ourselves to this case. From Eq. 1 it follows that we are discussing a high-finesse cavity.

THE NONLINEAR CAVITY EQUATION

For concreteness we now consider a *cylindrical* Fabry-Perot cavity consisting of two mirrors, one planar and the other concave and cylindrical [14], as shown in Fig. 1. Let x lie along the cylindrical mirror axis, z along the cavity longitudinal axis (normal to the plane mirror), and y along the other transverse direction, along which the cylindrical mirror is curved. The cavity interior is filled with a Kerr-type nonlinear medium ($\Delta n = n_2|\mathcal{E}|^2$). Assume that the mode frequency spacings in the z and y dimensions are larger than the laser linewidth and τ_{nl}^{-1} , so that in z and y only a single mode is occupied and the field dynamics in these directions is effectively eliminated; under these conditions we call the cavity *one-dimensional*, since spatial soliton formation occurs only along the x axis.

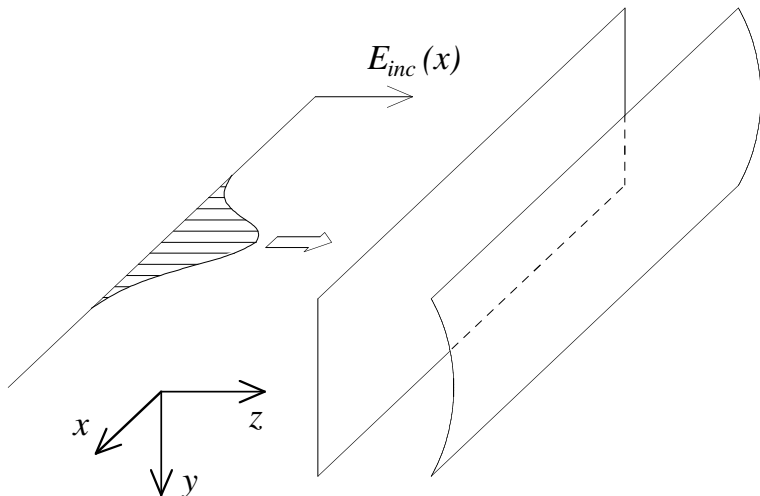


FIG. 1. Cylindrical Fabry-Perot resonator and associated coordinate system

The equation governing the evolution of the cavity’s internal field envelope is

$$\frac{\partial \mathcal{E}}{\partial t} = \frac{ic}{2k} \frac{\partial^2 \mathcal{E}}{\partial x^2} - \Gamma' \mathcal{E} + i(\Delta\omega') \mathcal{E} + \Gamma' \mathcal{E}_{drive} + i\omega n_2 |\mathcal{E}|^2 \mathcal{E}, \quad (3)$$

where \mathcal{E} is the internal cavity field amplitude, $k = 2\pi/\lambda$ is the longitudinal wavenumber, $\Gamma' = cT/L$ is the amplitude decay rate from the cavity (T is the amplitude transmission coefficient at each mirror, assumed equal, and L is the

cavity length), ω is the field angular frequency, $\Delta\omega' = \omega - \omega_{cav}$ is the detuning of the driving field from linear cavity resonance, and n_2 is the nonlinear index inside the cavity. This equation is the time-dependent version of that found by Haelterman *et al* from their modal theory [15].

We now make this equation dimensionless by choosing an arbitrary distance scale x_0 and relating the time and field scales t_0 and $|\mathcal{E}_0|$ to it using $t_0 = kx_0^2/c$ and $|\mathcal{E}_0| = 1/kx_0\sqrt{|n_2|}$. After rescaling Eq. 3 takes on the dimensionless form

$$\dot{\Psi} = \frac{i}{2}\nabla^2\Psi + i\sigma|\Psi|^2\Psi + i\Delta\omega\Psi - \Gamma(\Psi - \Psi_{drive}), \quad (4)$$

where $\sigma = +1(-1)$ for self-focusing (-defocusing), $\Psi = \mathcal{E}/|\mathcal{E}_0|$, $\Delta\omega = \Delta\omega't_0$, and $\Gamma = \Gamma't_0$. The conditions of Eq. 2 have allowed us to use the mean-field limit in deriving this equation and also imply that $\Gamma \ll 1$.

The external incident, transmitted, and reflected fields are related to the internal fields of Eq. 4 by

$$\begin{aligned} \Psi_{inc} &= T\Psi_{drive} \\ \Psi_{trans} &= T\Psi \\ \Psi_{refl} &= iT\sqrt{1-T^2}(\Psi_{drive} - e^{-i\theta_{RT}}\Psi) . \end{aligned} \quad (5)$$

where θ_{RT} is the cavity round-trip phase accumulation calculated from Eq. 4,

$$\theta_{RT}(x) = \frac{2T}{\Gamma} \left(\Delta\omega + \sigma|\Psi|^2 + \frac{1}{|\Psi|^2} \text{Im} \left\{ \Psi^* \left(\frac{i}{2}\nabla^2\Psi + \Gamma\Psi_{drive} \right) \right\} \right), \quad (6)$$

and we have assumed the mirrors are lossless. Equations 4-6 provide a complete framework for calculating the transmission and reflection properties of the cylindrical nonlinear Fabry-Perot cavity.

SOLITON FILTERING AND THE OPTICAL WHISTLE

Equation 4 is a damped, driven version of the nonlinear Schrodinger equation (NLSE). In the limit $\Gamma \rightarrow 0$ and for $\sigma = +1$ it admits the family of stationary soliton solutions

$$\begin{aligned} \Psi(X, T) &= d^{-1} \text{sech}(X/d) \\ \Delta\omega &= -1/(2d^2) \end{aligned} \quad (7)$$

where d is an arbitrary width and $X = x/x_0$, $T = t/t_0$ are dimensionless coordinates. There are other, time-dependent (“breather”), soliton solutions [16] which are unimportant for our present purposes. Equation 7 is also a solution in the damped case ($\Gamma \neq 0$) if the driving field has the special form

$$\Psi_{drive, sech}(X, T) = \Psi(X, T) = d^{-1} \text{sech}(X/d) . \quad (8)$$

A general qualitative feature of solitons is their robustness to small perturbations. With this in mind, we might expect that the Gaussian driving field

$$\Psi_{drive, Gaussian}(X, T) = d^{-1} \exp \left[-X^2/(1.699d)^2 \right] . \quad (9)$$

may lead to the soliton solution (7) nearly as efficiently as the sech drive (8). The constant 1.699 has been chosen to minimize the difference integral

$$\int_{-\infty}^{\infty} [\Psi_{drive, Gaussian}(X) - \Psi_{drive, sech}(X)]^2 dx . \quad (10)$$

This possibility was considered in a travelling-wave geometry by Burak and Nasalski [17], who found that as much as 99.5% of the incident power is converted into a soliton.

In our present situation it is found that the folded path arising from the cavity configuration can modify this picture substantially. Generally, soliton-forming behavior is observed when the driving field amplitude is matched to its width, as in Eq. 9. Because the non-soliton incident beam profile yields a soliton beam in transmission, we call this process *soliton filtering* in analogy with ordinary spatial filtering. A larger driving amplitude leads to a “mode-mismatch” since the soliton is trying to form with a smaller width than the input beam. The optical whistle oscillation results from a competition between the soliton trying to shrink in size, and the driving field feeding in light mismatched in phase and spatial profile.

Considering again the Gaussian driving field of Eq. 9, recall that the choice of distance scale x_0 in deriving Eq. 4 is arbitrary, so that we can choose it to be the waist size of the input beam without loss of generality. (In this case the time scale t_0 is the time of flight through the beam's Rayleigh range.) Then we have $\Psi_{drive}(X, T) = q \exp(-X^2)$ where q is a real, dimensionless driving amplitude, and our model is characterized by the four dimensionless quantities σ , Γ , $\Delta\omega$, and q . We expect optimal coupling into the soliton when

$$\begin{aligned} q &\approx 1.699 \\ \Delta\omega &\approx -(1.699)^2/2 = -1.443. \end{aligned} \quad (11)$$

The former is remarkably close to the optimal value 1.69 in the travelling-wave case, found using the inverse scattering transform [17].

NUMERICAL TECHNIQUE

As previously noted, when $\Gamma = 0$ Equation 4 is the NLSE, efficiently solved using a modified split-step Fourier method. The basic split-step technique [18] [19] evaluates the Laplacian diffraction term in Fourier space and the nonlinear $|\Psi|^2$ term in real space. By dividing these properly, one gets accuracy through two orders in the time step size h (the leading order error *per step* is $O(h^3)$). The method is modified to solve our more general problem by first writing Eq. 4 in the form

$$\dot{\Psi} = \hat{a}\Psi + b, \quad (12)$$

where the operator \hat{a} is written as the sum of linear and nonlinear parts, $\hat{a} = \hat{l} + \hat{n}$, and

$$\begin{aligned} \hat{l} &= \frac{i}{2}\nabla^2 - \Gamma + i\Delta\omega \\ \hat{n} &= i\sigma|\Psi|^2 \\ b &= \Gamma\Psi_{drive}. \end{aligned}$$

In the case $b = 0$ the split-step technique gives

$$\Psi(t + h) \equiv e^{h\hat{a}}\Psi(t) = e^{\frac{1}{2}h\hat{l}}e^{h\hat{n}}e^{\frac{1}{2}h\hat{l}}\Psi(t) + O(h^3), \quad (13)$$

which is easily verified by expanding the exponentials in their respective Taylor series. To solve the general problem ($b \neq 0$) to the same order in h , we begin by writing $\Psi(t + h)$ as a Taylor series in h :

$$\Psi(t + h) = \Psi(t) + h\dot{\Psi}(t) + \frac{1}{2}h^2\ddot{\Psi}(t) + \dots \quad (14)$$

Equation 12 gives $\dot{\Psi}(t)$, and upon taking the derivative with respect to time we find:

$$\begin{aligned} \ddot{\Psi}(t) &= \hat{l}\left[(\hat{l} + i\sigma|\Psi|^2)\Psi + b\right] + i\sigma\left\{2|\Psi|^2\left[(\hat{l} + i\sigma|\Psi|^2)\Psi + b\right]\right. \\ &\quad \left. + \Psi^2\left[(\hat{l}^* - i\sigma|\Psi|^2)\Psi^* + b^*\right]\right\} + \dot{b}, \end{aligned} \quad (15)$$

where we have explicitly written out \hat{n} to help in taking the derivative ($\dot{n} \neq 0$). Substituting $\dot{\Psi}$ and $\ddot{\Psi}$ into Eq. 14 and using the relation $\dot{b}(t) = [b(t + h) - b(t)]/h + O(h)$ yields

$$\begin{aligned} \Psi(t + h) &= \Psi(t + h)|_{b=0} \\ &\quad + \frac{1}{2}h[b(t) + b(t + h)] + \frac{1}{2}h^2\left[\hat{l}b + i\sigma(2|\Psi|^2b + \Psi^2b^*)\right] \\ &\quad + O(h^3). \end{aligned} \quad (16)$$

The first term on the right is done using the split-step method (Eq. 13), and the remaining two terms add on the effects of the driving field. The time-dependent terms (Ψ , b , b^*) appearing in the h^2 driving term can be evaluated at any point between times t and $t + h$, and accuracy through second order in h will be retained.

The results presented below were calculated using a time step h of 0.01 and a spatial grid consisting of 256 points separated by 0.156 dimensionless units. Although the latter may seem high (relative to the incident beam waist of 1.0), the split-step method performs admirably in this regard since it performs all derivatives in frequency space. These values were found to give accurate results for the cases of interest here; halving the grid spacings in space and time yielded essentially identical results for a variety of test cases.

RESULTS

Figure 2 summarizes the asymptotic (long-time) cavity solutions when the Gaussian driving field is suddenly turned on at $t = 0$. We have here assumed an initially empty cavity, $\sigma = +1$, and $\Gamma = 0.14$. In this figure the asymptotic cavity solutions are categorized into five basic types: (1) steady-state solutions, (2) period 1 oscillations, (3) period 2 oscillations, (4) long-period oscillations, and (5) chaotic (intermittent) oscillations. The regions are seen to have complex boundaries, and points near the borders of the “chaotic” regions show particularly interesting behaviors: at the borders with steady-state regions lie oscillations of very long period, and at the borders with the normal oscillating regions there is evidence of period-doubling. Period 3 oscillations have also been observed. Time series of examples are shown in Figure 3, where we plot the total power output for a variety of cases. For the period 1 example, snapshots of the cavity field amplitude are shown in Figure 4. The field profile narrows as the soliton forms, then is attenuated as the nonlinearity shifts the peak out of cavity resonance and power enters at the edges.

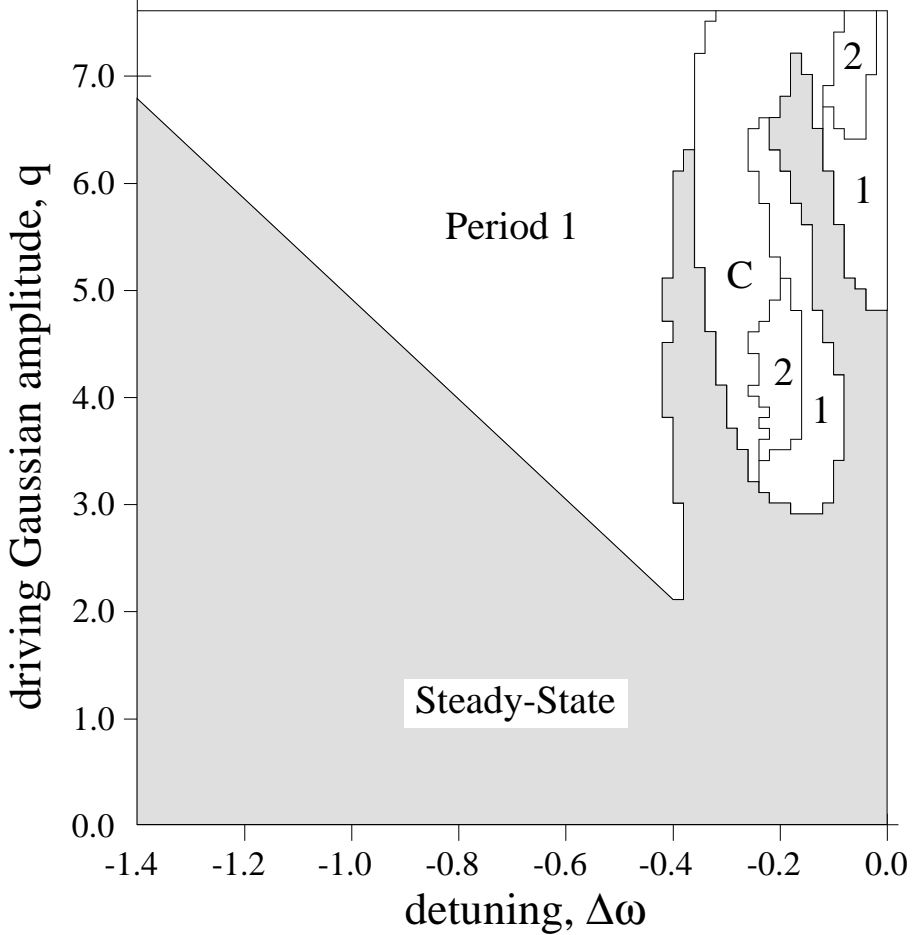


FIG. 2. Asymptotic behavior of cavity field, for $\sigma = +1$, $\Gamma = 0.14$, and an initially empty cavity. Labels indicate regions of steady-state, period 1 oscillation (1), period 2 oscillation (2), and chaos (C).

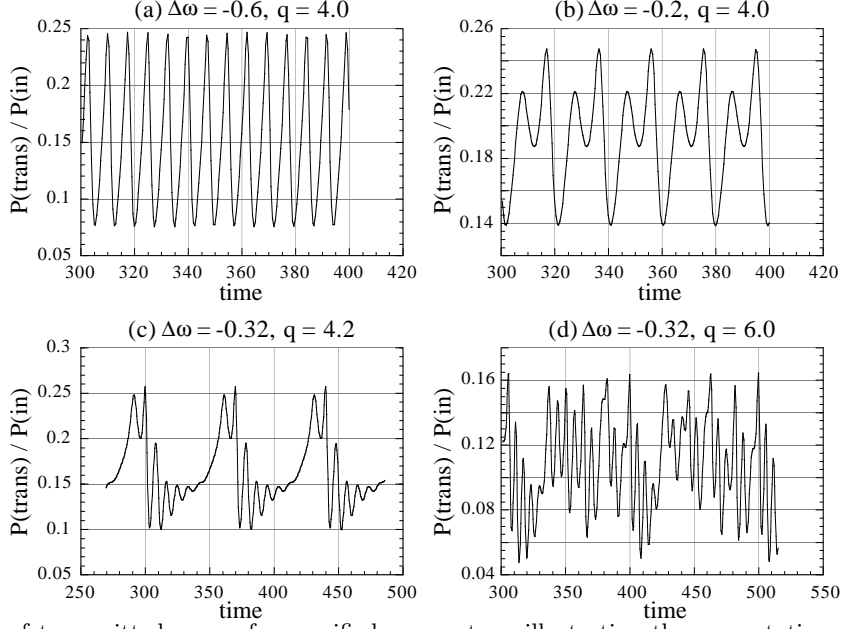


FIG. 3. Time series of transmitted power for specified parameters, illustrating the asymptotic solutions shown in Fig. 2. $\sigma = +1$ and $\Gamma = 0.14$.

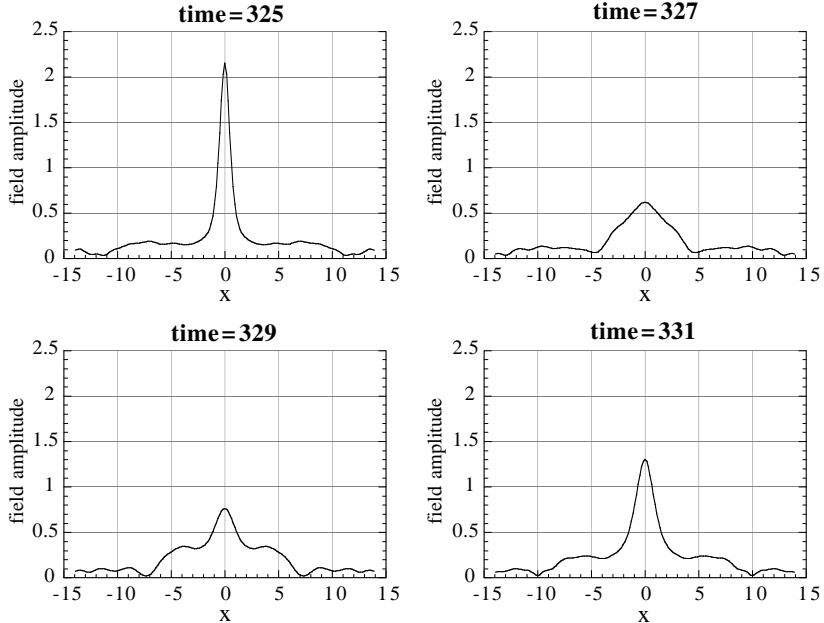


FIG. 4. Cavity field amplitude profiles for the period 1 oscillation shown in Figure 3. $\Delta\omega = -0.6$, $q = 4.0$.

An interesting issue is the effect the optical whistle has on optical bistability. Figure 5 compares a bistability curve from our time-dependent analysis with that given in Ref. [20] which assumed a steady-state field. Our respective equations have been made dimensionless in slightly different manners; to correspond to the $X_0 = 1$, $\Delta = +3$ curve in their Figure 3a we have chosen $\Gamma = X_0^2/2 = 0.5$, $\Delta\omega = -\Gamma\Delta = -1.5$ and have related their field amplitude f to ours using $\Psi = \sqrt{\Gamma}f$. Part of the upper branch of the bistability curve is seen to be unstable due to the whistle oscillation, and the oscillation amplitude is indicated by the bars in Fig. 5. In general we observe that, where bistability occurs ($\Delta\omega < -0.19$ for our choice $\Gamma = 0.14$) the whistle oscillation occurs only in the upper branch of the bistability curve. However, the whistle can also occur when there is no bistability, as is evident from Fig. 2.

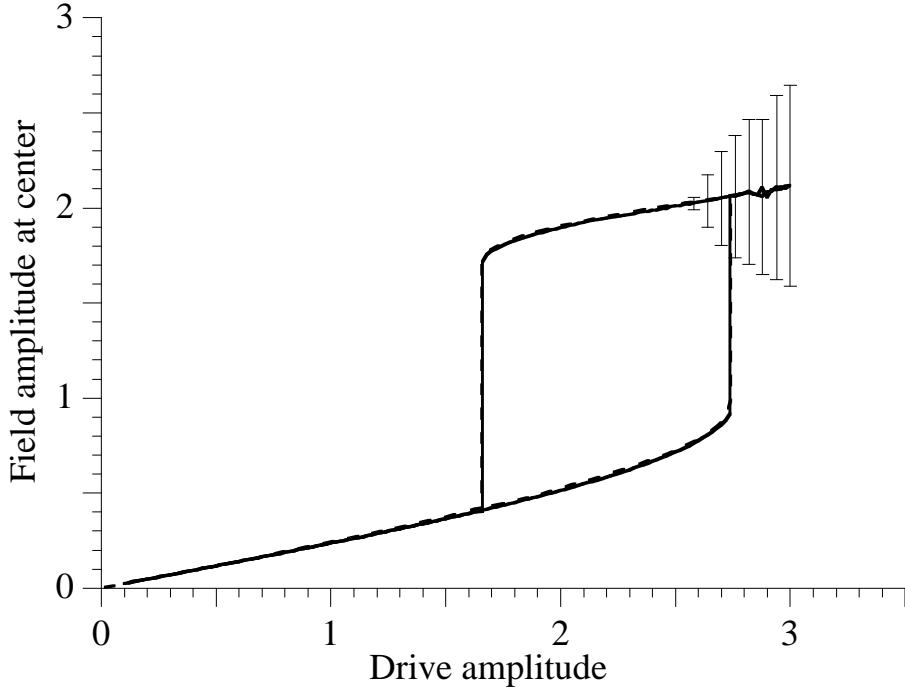


FIG. 5. Comparison with steady-state theory. The dashed bistability curve is from Fig. 3a of Vitrant *et al* (1990) and the solid curve is from our time-dependent analysis. Bars on the solid curve show the oscillation amplitude. $\Gamma = 0.5$, $\Delta\omega = -1.5$.

In other cases the optical whistle modifies bistability curves more drastically. Figure 6 shows steady-state and time-dependent bistability curves for $\Gamma = 0.14$, $\Delta\omega = -1.443$. In this case the whistle oscillation has moved the switch-off point substantially, a common occurrence. In contrast, the switch-on point has not been seen to change from its steady-state value in our analysis.

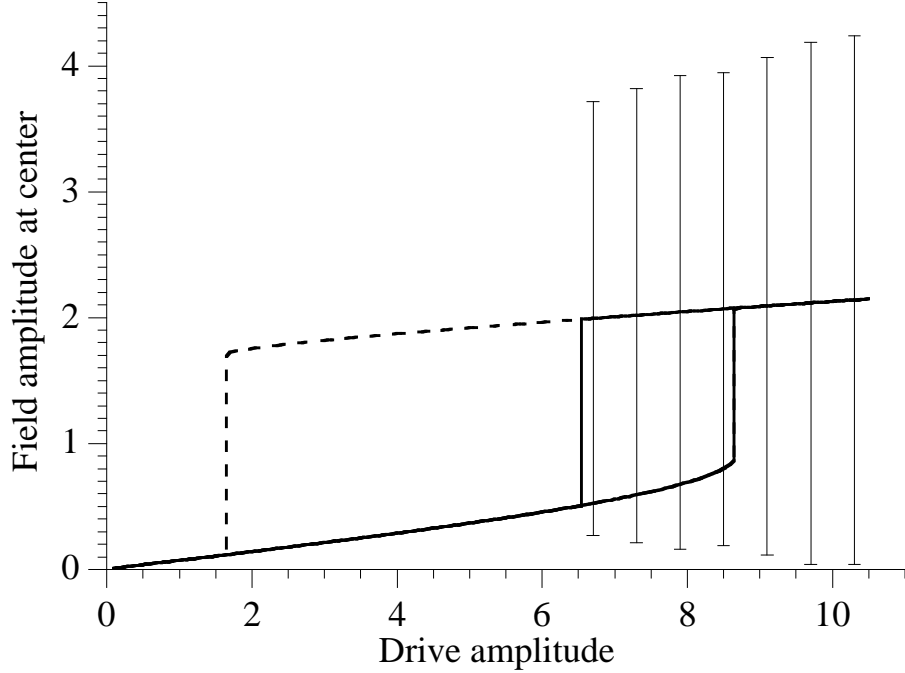


FIG. 6. Comparison of steady-state (dashed) and time-dependent (solid, with oscillation amplitude indicated by bars) analyses. In this case the whistle instability changes the switch-off point in the bistability curve. $\Gamma = 0.14$, $\Delta\omega = -1.443$.

Spatial soliton formation within the cavity is our final topic of consideration. In the travelling-wave case soliton formation with Gaussian driving beams can be very efficient; as much as 99.5% of the input power can be transformed

into a soliton [17]. In a cavity we might expect this to be an upper bound since imperfect interference (and reflection of the incident beam) would seem to present an additional loss of efficiency. In Eq. 11 we made a simple estimate of the optimal coupling parameters. However, Fig. 6 shows that for $\Delta\omega = -1.443$, $\Gamma = 0.14$ the whistle disrupts the bistability curve's upper branch near $q = 1.699$. A nearby case ($\Delta\omega = -1.2$, $\Gamma = 0.14$) without the disruption is shown in Fig. 7. At the switch-off point $q \approx 1.6$ the coupling efficiency into the transmitted soliton is 97.6%, still quite high. Because $\Gamma = 0.14 \ll 1$ the transmitted field is found to be quite close to the soliton form of Eq. 7; when $\Gamma > 1$ the transmitted field is more Gaussian in profile. For the present work we have not attempted a thorough study to optimize soliton coupling efficiency but simply wish to demonstrate that fairly high efficiencies are possible in cavities.

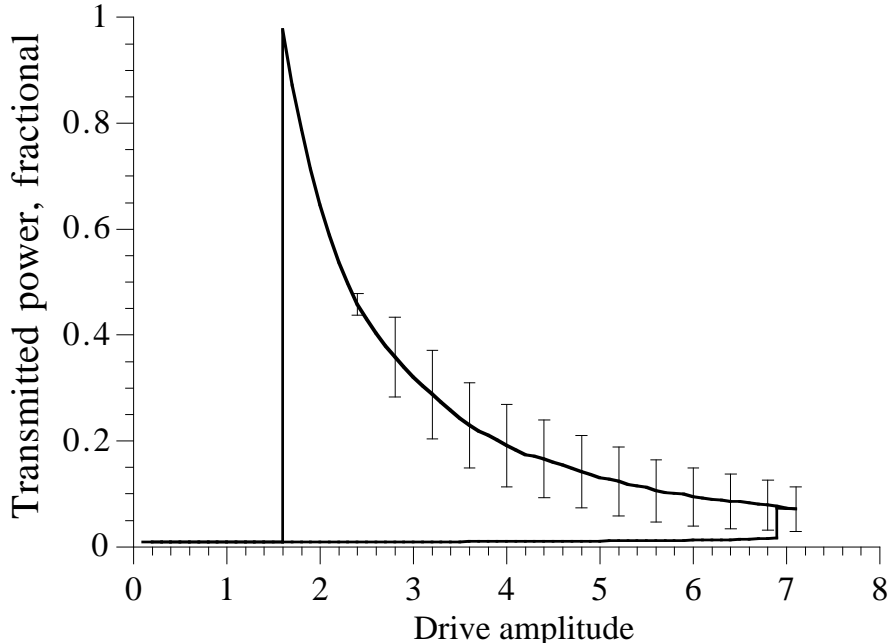


FIG. 7. Bistability curve showing nearly complete (97.6%) coupling into the spatial soliton. The expected optimal case, Eq. 11, is disrupted by the whistle as shown in Fig. 6. $\Delta\omega = -1.2$, $\Gamma = 0.14$.

DISCUSSION

A variety of oscillation phenomena similar to the optical whistle have been reported in the literature [1]. These can be broadly categorized into multi-mode and single-mode (mean field) effects. In the former case the plane-wave oscillation phenomenon has been called “self-pulsing” (it occurs in both the context of absorptive [21] and dispersive [5] [22] bistability). The instability here is essentially due to the interplay of two different timescales, nonlinearity and cavity feedback, and gives rise to an oscillation period which is a multiple of the cavity round-trip time. Slightly later the single-mode case was also shown to yield oscillations. Ikeda and Akimoto [23] first demonstrated this within a plane-wave, purely dispersive Kerr model. Lugiato *et al* [24] constructed a more realistic optical Bloch model and found oscillations (and chaos) in that case as well, again at the plane-wave level of description.

Our work is more closely related to the transverse instability discovered by McLaughlin *et al* [6] and discussed in the mean-field limit by Lugiato and Lefever [25]. In these studies transverse structure in a broad illuminating beam arises from a modulational instability. More recent numerical work has shown that these perturbations grow to become soliton chains [26] [7] which may or may not be stationary in time. For a plane-wave driving field of varying intensity a series of bifurcations similar to the ones seen here are observed to occur, eventually leading to spatio-temporal chaos [27]. Our present work is different because here the most unstable transverse wavelength is comparable to the driving field width; the instability consists of a broad spectrum of transverse wavenumbers and it is somewhat more intuitive to view the process as a mode mismatch in the soliton formation process rather than as a sinusoidal modulation in a very broad beam growing into a (perhaps) time-varying soliton chain.

The optical whistle phenomenon presented here is believed to exist beyond the Kerr-nonlinear, cylindrical Fabry-Perot model, whenever one is in the *soliton-forming limit* of Eq. 2. We conjecture this on the basis of our general picture that the whistle is the result of a mode mismatch between the generated soliton and driving field. The study

of related phenomena in other systems would be an interesting topic of further research.

ACKNOWLEDGEMENTS

The authors would like to thank Morgan W. Mitchell and Prof. Ewan M. Wright for very helpful discussions.

- [1] For a comprehensive review see R. Reinisch and G. Vitrant, *Prog. Quant. Electr.* **18**, 1 (1994).
- [2] W.J. Firth and A.J. Scroggie, *Phys. Rev. Lett.* **76**, 1623 (1996).
- [3] Q.A. Turchette, C.J. Hood, W. Lange, H. Mabuchi, and H.J. Kimble, *Phys. Rev. Lett.* **75**, 4710 (1995).
- [4] S.L. McCall, H.M. Gibbs, G.G. Churchill, and T.N.C. Venkatesan, *Bull. Am. Phys. Soc.* **20**, 636 (1975); S.L. McCall, H.M. Gibbs, and T.N.C. Venkatesan, *J. Opt. Soc. Am.* **65**, 1184 (1975).
- [5] K. Ikeda, *Opt. Commun.* **30**, 257 (1979).
- [6] D.W. McLaughlin, J.V. Moloney, and A.C. Newell, *Phys. Rev. Lett.* **54**, 681 (1985).
- [7] M. Haelterman and G. Vitrant, *J. Opt. Soc. Am. B* **9**, 1563 (1992).
- [8] T.B. Benjamin and J.E. Fier, *J. Fluid Mech.* **27**, 417 (1966).
- [9] R.Y. Chiao, E. Garmire, and C.H. Townes, *Phys. Rev. Lett.* **13**, 479 (1964).
- [10] S.A. Akhmanov, A.P. Sukhorukov, and R.V. Khokhlov, *Sov. Phys. JETP* **23**, 1025 (1966).
- [11] A.W. Snyder, D.J. Mitchell, and Yu.S. Kivshar, *Mod. Phys. Lett. B* **9**, 1479 (1995).
- [12] A.W. Snyder and Yu.S. Kivshar, *J. Opt. Soc. Am. B* **14**, 3025 (1997).
- [13] L.A. Lugiato and L.M. Narducci, *Z. Phys. B* **71**, 129 (1988).
- [14] I.H. Deutsch and R.Y. Chiao, *Phys. Rev. Lett.* **69**, 3627 (1992).
- [15] M. Haelterman, G. Vitrant, and R. Reinisch, *J. Opt. Soc. Am. B* **7**, 1309 (1990).
- [16] G.P. Agrawal, *Nonlinear Fiber Optics* (Academic Press, San Diego, 1989), p. 111.
- [17] D. Burak and W. Nasalski, *Applied Optics* **33**, 6393 (1994).
- [18] Ref. [16], p. 44.
- [19] T.R. Taha and M.J. Ablowitz, *J. of Comp. Phys.* **55**, 203 (1984).
- [20] G. Vitrant, M. Haelterman, and R. Reinisch, *J. Opt. Soc. Am. B* **7**, 1319 (1990).
- [21] R. Bonifacio, M. Gronchi, and L.A. Lugiato, *Opt. Comm.* **30**, 129 (1979).
- [22] L.A. Lugiato, *Opt. Comm.* **33**, 108 (1980).
- [23] K. Ikeda and O. Akimoto, *Phys. Rev. Lett.* **48**, 617 (1982).
- [24] L.A. Lugiato, L.M. Narducci, D.K. Bandy, and C.A. Pennise, *Opt. Comm.* **43**, 281 (1982).
- [25] L.A. Lugiato and R. Lefever, *Phys. Rev. A* **58**, 2209 (1987).
- [26] G.S. McDonald and W.J. Firth, *J. Opt. Soc. Am. B* **7**, 1328 (1990).
- [27] K. Nozaki and N. Bekki, *Physica* **21D**, 381 (1986).